

Regulation of Band 3 Rotational Mobility by Ankyrin in Intact Human Red Cells[†]Michael R. Cho,[‡] Stefan W. Eber,^{§,||} Shih-Chun Liu,[⊥] Samuel E. Lux,[§] and David E. Golan^{*,‡}

Departments of Biological Chemistry and Molecular Pharmacology, Medicine, and Pediatrics, Harvard Medical School, Hematology Division, Brigham and Women's Hospital, Division of Hematology–Oncology, Children's Hospital, Boston, Massachusetts 02115, Department of Biomedical Research, St. Elizabeth's Medical Center of Boston, Tufts University Medical School, Boston, Massachusetts 02135, and Universitäts-Kinderklinik, D-37075 Göttingen, FRG

Received July 29, 1998; Revised Manuscript Received October 19, 1998

ABSTRACT: Ankyrin mutations and combined spectrin and ankyrin deficiency are prominent features of red blood cells (RBCs) in patients with hereditary spherocytosis (HS). Band 3 is the most abundant integral protein in the human RBC membrane. Previous studies have shown that the lateral mobility, but not the rotational mobility, of band 3 is increased in RBCs from patients with severe autosomal recessive HS and selective spectrin deficiency. These observations are consistent with the steric hindrance model of lateral mobility restriction. Here we use the fluorescence photobleaching recovery and polarized fluorescence depletion techniques to measure the lateral and rotational mobility of band 3 in intact RBCs from six patients with HS, ankyrin mutations, and combined spectrin and ankyrin deficiency. As predicted by the steric hindrance model, the lateral diffusion rate of band 3 is greater in spectrin- and ankyrin-deficient RBCs than in control cells, and the magnitude of the increase correlates with the degree of spectrin deficiency. Unlike RBCs from patients with HS and selective spectrin deficiency, however, HS RBCs with ankyrin mutations exhibit a marked increase in band 3 rotational diffusion. The magnitude of the increase correlates inversely with the ankyrin/band 3 ratio and with the fraction of band 3 retained in the membrane skeleton following detergent extraction. These data suggest that ankyrin deficiency relaxes rotational constraints on the major (slowly rotating) population of band 3 molecules. Increases in band 3 rotation could be due to release of band 3 from low-affinity binding sites on ankyrin.

The intact human red blood cell (RBC)¹ provides a biochemically characterized biological membrane for detailed studies of the molecular interactions that control the lateral and rotational mobility of transmembrane proteins. The RBC membrane consists of a lipid bilayer, in which transmembrane proteins are embedded, and a membrane skeleton that laminates the inner bilayer surface. Spectrin, actin, and protein 4.1 are the major components of the membrane skeleton. The skeleton is mechanically coupled to the lipid bilayer through multiple protein–protein interactions involving membrane skeletal proteins, linking proteins, and trans-

membrane proteins (1–3). Mechanical coupling is critical for maintenance of RBC membrane strength and flexibility (4–8). Band 3, which represents approximately 30% of the RBC membrane protein, is the transmembrane anion exchanger (9–11). The cytoplasmic domain of band 3 provides binding sites for the linking proteins ankyrin (12–14), protein 4.1 (15, 16), and protein 4.2 (17–19). In turn, these linking proteins bind with high and/or low affinity to spectrin (20–24).

In the fluid mosaic membrane model (25), the lateral and rotational mobilities of transmembrane proteins are determined by the size and shape of the proteins and by the viscosity of the lipid bilayer. In biological membranes, however, other molecular interactions are likely to impose constraints on mobility (26–28). Such constraints include interactions among transmembrane proteins, interactions between transmembrane proteins and cytoskeletal or membrane skeletal proteins, and interactions between transmembrane proteins and laterally segregated domains of plasma membrane lipid (28). In normal human RBCs, band 3 lateral diffusion coefficients are $(1–2) \times 10^{-11} \text{ cm}^2 \text{ s}^{-1}$, and band 3 fractional mobilities are 40–70% (29–32). Band 3 appears to rotate in normal human RBC membranes as three distinct molecular species: 20–25% of band 3 molecules rotate rapidly (rotational relaxation time $\tau < 250 \mu\text{s}$), 50–75% rotate slowly ($\tau \sim 1–3 \text{ ms}$), and 5–25% are rotationally immobile (31–35). Both the lateral and rotational mobilities of band 3 are constrained significantly in normal human RBCs, because band 3 molecules released from membrane

[†] This work was supported by National Institutes of Health Grants HL-32854 and HL-15157 (D.E.G.) and DK-34083 and HL-32262 (S.E.L.), and by Deutsche Forschungsgemeinschaft Grants Eb 99/1-3 and Eb 99/3-1+2 (S.W.E.).

* Address correspondence to this author at the Department of Biological Chemistry and Molecular Pharmacology, Harvard Medical School, 250 Longwood Ave., Boston, MA 02115. Telephone: (617) 432-2256. FAX: (617) 432-3833. E-mail: degolan@warren.med.harvard.edu.

[‡] Departments of Biological Chemistry and Molecular Pharmacology and of Medicine, Harvard Medical School, Hematology Division, Brigham and Women's Hospital.

[§] Department of Pediatrics, Harvard Medical School, Division of Hematology–Oncology, Children's Hospital.

^{||} Universitäts-Kinderklinik.

[⊥] Department of Biomedical Research, Tufts University Medical School.

¹ Abbreviations: C₁₂E₈, octaethylene glycol *n*-dodecyl monoether; ELISA, enzyme-linked immunosorbent assay; EMA, eosin-5-maleimide; HS, hereditary spherocytosis; HS^{ank}, HS with combined spectrin and ankyrin deficiency; HS^{sp}, HS with selective spectrin deficiency; KPBS, high potassium phosphate-buffered saline; RBC, red blood cell.

Table 1: Spectrin, Ankyrin, and Band 3 Content of HS^{ank} RBCs^a

sample	spectrin content (copies per RBC)	ankyrin content (copies per RBC)	band 3 content (copies per RBC)	sp/band 3 ratio	ank/band 3 ratio
patient 1	161 000	95 000	900 000	0.73	0.82
patient 2	165 000	98 000	780 000	0.86	0.98
patient 3	130 000	73 000	680 000	0.78	0.84
patient 4	156 000	92 000	777 000	0.82	0.93
patient 5	152 000	92 400	649 000	0.96	1.11
patient 6	190 000	95 900	658 000	1.18	1.14
normal RBCs	224 000 ± 29 000	117 000 ± 10 000	914 000 ± 130 000	1.00	1.00

^a Patients 1 and 2 were heterozygous for a single ankyrin-1 gene deletion; patients 3, 4, and 5 were heterozygous for a frameshift mutation in one ankyrin-1 gene and did not express the variant ankyrin; patient 6 was a compound heterozygote for a base pair substitution in the promoter region of one ankyrin-1 gene and a base pair substitution in the exon 13 region of the other ankyrin-1 gene, and did express both native and variant ankyrin. Protein content was measured by ELISA. Spectrin/band 3 (sp/band 3) and ankyrin/band 3 (ank/band 3) ratios were normalized to protein ratios in normal RBCs, computed on the basis of measurements of protein content in normal RBCs. Replicate determinations from the same normal or HS^{ank} individual yielded a standard deviation of about 5% of the mean value for spectrin, ankyrin, and band 3 content. Normal RBC spectrin, ankyrin, and band 3 content values represent mean ± standard deviation.

skeletal constraints or reconstituted in artificial bilayer membranes exhibit significantly larger lateral diffusion coefficients of $5 \times 10^{-10} \text{ cm}^2 \text{ s}^{-1}$ and shorter τ values of 25–50 μs (29, 32, 36, 37).

In normal RBCs, the lateral diffusion of mobile band 3 molecules is slowed primarily by steric hindrance interactions between the cytoplasmic domain of band 3 and the spectrin-based membrane skeleton (29, 37–40). We have shown that the lateral diffusion rate of band 3 is inversely related to the spectrin content of the membrane in RBCs from patients with severe autosomal recessive hereditary spherocytosis (HS) and selective spectrin deficiency (HS^{sp}) (32). Interestingly, the rotational mobility of band 3 in HS^{sp} RBCs is identical to that in normal RBCs. These data provide strong support for a model in which band 3 lateral mobility is constrained by steric interactions with the membrane skeleton.

The rapidly rotating band 3 fraction is presumed to consist of free band 3 dimers, tetramers, and possibly higher order oligomers (34, 36). In some pathologic RBCs, the rotationally immobile band 3 fraction contains clustered or linearly aggregated band 3 molecules (31, 41–43), but in normal cells this fraction is likely to represent band 3 molecules bound with high affinity to ankyrin. The slowly rotating band 3 fraction is less well characterized, however. Low-affinity binding interactions between band 3 and membrane skeletal proteins such as ankyrin (44, 45), protein 4.1 (15), and protein 4.2 (18, 19, 24) may be involved in rotational mobility constraints. To investigate directly and specifically the role of ankyrin in controlling band 3 rotational mobility, we have identified a panel of six patients with HS who have, in addition to spectrin deficiency, ankyrin deficiency and band 3 deficiency (HS^{ank}) (46). By using the fluorescence photobleaching recovery and polarized fluorescence depletion techniques, we have measured band 3 lateral and rotational mobility in RBCs from HS^{ank} patients. Such cells manifest the increased band 3 lateral diffusion rates characteristic of spectrin-deficient RBCs such as those from patients with HS^{sp}. Unlike HS^{sp} RBCs, however, HS^{ank} cells exhibit a striking increase in band 3 rotational mobility. These observations suggest that ankyrin regulates band 3 rotational mobility not only through high-affinity binding interactions between ankyrin and a relatively small population of rotationally immobile band 3 molecules, but also through low-affinity binding interactions between ankyrin and the major population of slowly rotating band 3 molecules.

MATERIALS AND METHODS

Patients. Genetic defects in the six HS^{ank} patients have been characterized and reported elsewhere. Two patients (patients 1 and 2; Table 1) were heterozygous for a single ankyrin-1 gene deletion (47). Three patients were heterozygous for a frameshift mutation in one ankyrin-1 gene [patients 3 and 4, a 4 nt deletion (TTAGTC → TC) in codons 797–798; patient 5, a 1 nt deletion (ACA → AA) in codon 1127], and did not express the variant protein (46). One patient was a compound heterozygote for a base pair substitution in the promoter region of one ankyrin-1 gene (T → C, 108 nt before the translation start site) and a base pair substitution in the exon 13 region of the other ankyrin-1 gene (Val 463 → Ile, GTC → ATC), and did express both native and variant protein (46, 48). Patients 1 and 2 were sisters; patients 3 and 4 were mother and daughter; patients 5 and 6 were unrelated. RBC spectrin, ankyrin, and band 3 contents were measured by enzyme-linked immunosorbent assay (ELISA) (48). Unless otherwise noted, blood samples were collected in Germany, shipped on ice to Boston, MA, and processed for mobility measurements within 48 h.

Fluorescent Labeling of Band 3. Blood was washed 3 times in high potassium phosphate buffered saline (KPBS: 140 mM KCl, 15 mM NaPO₄, 10 mM glucose, pH 7.4). Band 3 was labeled by incubating 100 μL of packed RBCs with 40 μL of eosin-5-maleimide (EMA; 0.25 mg/mL in KPBS; Molecular Probes, Eugene, OR) for 12 min at room temperature. After incubation, cells were washed extensively in KPBS with 1% BSA. Under these conditions, >90% of the membrane-associated fluorescence was covalently bound to band 3 (30; unpublished observations).

Lateral Mobility Measurements. The fluorescence photobleaching recovery technique (49) was used to measure the lateral mobility of EMA-labeled band 3. Briefly, the 488 nm line from an argon ion laser of Gaussian spatial profile was selected and focused onto the microscope stage. A short (typically 100 ms) intense (typically 1 mW) laser pulse was used to photobleach a spot of 0.7 μm radius on the upper membrane of a single RBC. The fluorescence intensity of the bleached spot was then monitored by using periodic low intensity (typically 0.1 μW) laser pulses. Fluorescence recovery resulted from the lateral diffusion of unbleached fluorophores into the bleached area. A nonlinear least-squares fitting procedure (50) was used to determine the lateral

diffusion coefficient (D) and fractional mobility (f) of band 3 molecules from the fluorescence recovery data. Effects of cell shape on fluorescence recovery kinetics were negligible, because intracellular hemoglobin effectively shielded the lower membrane from excitation laser light and emitted fluorescence (unpublished observations). Details of the optics and electronics of our apparatus have been described (31). All measurements were performed at 37 °C. The local temperature rise during the bleaching pulse because of laser-induced heating of surface fluorophores was calculated (51) to be <0.02 °C, and that because of heating of intracellular hemoglobin to be 0.03 °C.

Rotational Mobility Measurements. The polarized fluorescence depletion technique (51) was used to measure the rotational mobility of EMA-labeled band 3. In a typical polarized fluorescence depletion experiment, a diffuse laser beam (typically 30 μm in radius) was used to illuminate approximately 40 RBCs, data were collected, and the microscope slide was translated in order to illuminate a new field of RBCs. Data were accumulated (pooled) from approximately 500 RBCs in each sample, so the data represented the average rotational mobility of approximately 5×10^8 band 3 molecules. EMA was anisotropically excited to the triplet state by a short (typically 10 μs), intense (typically 100 mW), polarized photoselection laser pulse. The fluorescence intensity of ground state molecules was monitored in two orthogonal directions by using polarized low intensity (typically 10 μW) laser pulses. Recovery of ground-state fluorescence following photoselection resulted from triplet decay and from rotational diffusion of EMA-labeled band 3 (34, 51, 52). The decay of ground-state fluorescence anisotropy, $r(t)$, was analyzed by using a nonlinear least-squares method and fitted to the equation:

$$r(t) = \alpha \exp(-t/\tau_1) + \beta \exp(-t/\tau_2) + r(\infty)$$

where α and β were the fractions of band 3 associated with the characteristic rotational relaxation times τ_1 (rapidly rotating phase) and τ_2 (slowly rotating phase), respectively. $r(\infty)$ was the residual anisotropy, reflecting the fraction of rotationally immobile band 3. In no case were more than two exponential terms required to fit anisotropy decay data adequately. Some anisotropy decay data were adequately fitted according to a single rotationally mobile phase. In the latter cases, β was set to 0. Adequacy of fit was assessed by the minimum number of exponential terms required to produce no significant change in the chi-square statistic. Because oxygen effectively quenches the excited triplet state of EMA, it was necessary to deoxygenate RBCs prior to rotational mobility measurements. EMA-labeled cells were deoxygenated in a nitrogen chamber for 60 min, and then treated with an enzyme oxygen scavenging system consisting of 50 units/mL glucose oxidase, 20 mM glucose, and 104 units/mL catalase (52). All measurements were performed at 37 °C.

Band 3 Extractability from RBC Membranes by the Nonionic Detergent Octaethylene Glycol *n*-Dodecyl Monoether ($C_{12}E_8$). RBC ghosts (3 mg of protein/mL) were prepared by hypotonic lysis and mixed with equal volumes of 0.5% $C_{12}E_8$ in isotonic buffer (150 mM NaCl, 5 mM NaPO_4 , pH 7.4) for 10 min at 4 °C. After centrifugation at 150000g for 30 min, the supernatants and pellets were

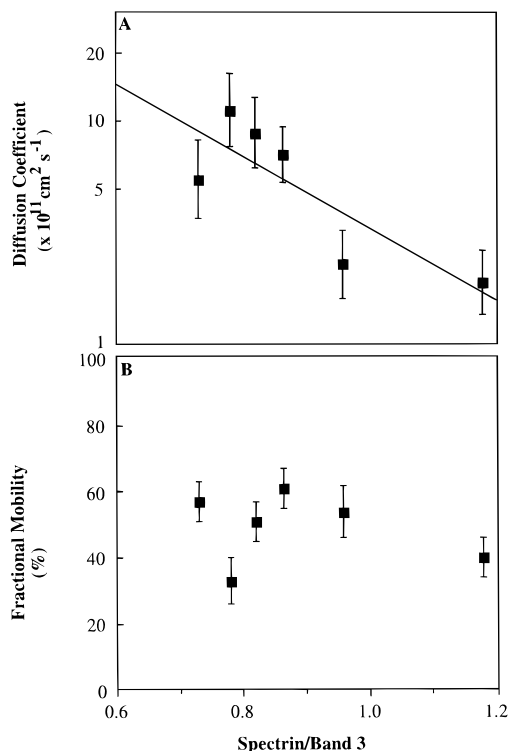


FIGURE 1: Dependence of the lateral diffusion coefficient (A) and fractional mobility (B) of band 3 on the normalized spectrin/band 3 ratio in intact RBCs from HS^{ank} patients. Each data point represents the mean (\pm SD) value of independent measurements on 8–12 cells from each patient. (A) Equation of best fit was: $\ln(\text{diffusion coefficient}) = 4.9 - 3.7(\text{spectrin/band 3})$; $R^2 = 0.68$. (B) The fraction of laterally mobile band 3 was independent of the normalized spectrin/band 3 ratio.

analyzed by SDS–PAGE according to Agre et al. (53). The band 3/spectrin ratio was analyzed by densitometric gel scanning, and normalized by the ratio obtained in ghost membranes to obtain the percent of total band 3 retained in $C_{12}E_8$ -extracted isotonic skeletal shells.

RESULTS

ELISA analysis indicated that RBCs from all six HS^{ank} patients manifested not only spectrin deficiency but also ankyrin deficiency and band 3 deficiency. Spectrin content was 58–85% of normal; ankyrin content was 62–84% of normal; and band 3 content was 71–98% of normal. Normalized against the corresponding ratios in normal RBCs, spectrin/band 3 and ankyrin/band 3 ratios were 0.73–1.18 and 0.82–1.14, respectively (Table 1).

The fluorescence photobleaching recovery technique was used to measure the lateral mobility of EMA-labeled band 3. Band 3 lateral diffusion coefficients in normal RBCs were $(1.6 \pm 0.4) \times 10^{-11} \text{ cm}^2 \text{ s}^{-1}$ (mean \pm SD, $n = 4$ individuals), similar to previously reported values (29, 31, 32, 40, 43, 45, 54–57). The lateral diffusion coefficient of HS^{ank} band 3 was found to depend on the RBC spectrin/band 3 ratio. When the logarithm of the band 3 diffusion coefficient was plotted against the spectrin/band 3 ratio, an inverse linear relationship was observed with $R^2 = 0.68$ (Figure 1A). Diffusion coefficients ranged from $1.9 \times 10^{-11} \text{ cm}^2 \text{ s}^{-1}$, at a spectrin/band 3 ratio of 1.14, to $11 \times 10^{-11} \text{ cm}^2 \text{ s}^{-1}$, at a spectrin/band 3 ratio of 0.84. The extrapolated diffusion coefficient at 0% spectrin was $130 \times 10^{-11} \text{ cm}^2 \text{ s}^{-1}$, which is of the

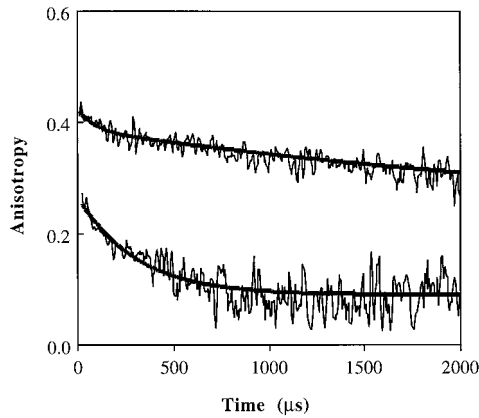


FIGURE 2: Anisotropy decay curves showing band 3 rotational mobility in normal (upper curve) and HS^{ank} (lower curve) RBCs. The anisotropy decay curve for the normal RBCs was offset by +0.2 unit for clarity. Normalized ankyrin/band 3 ratios in the normal and HS^{ank} samples were 1.0 and 0.93, respectively. Data from approximately 500 cells were collected to obtain each curve. Band 3 rotational mobility was markedly different in normal and HS^{ank} RBCs. Data were fitted to two exponentials for normal RBCs and to a single exponential for HS^{ank} RBCs. Control: $\alpha = 16\%$, $\tau_1 = 83 \mu\text{s}$, $\beta = 79\%$, $\tau_2 = 3.5 \text{ ms}$, $r(\infty) = 5\%$. HS^{ank}: $\alpha = 78\%$, $\tau = 307 \mu\text{s}$, $r(\infty) = 22\%$.

same magnitude as the band 3 “rapid diffusion limit” previously observed in RBC ghosts (29, 30). Both the slope and the intercept of the regression line were similar to those observed for the dependence of the band 3 lateral diffusion coefficient on spectrin/band 3 ratio in HS^{sp} RBCs with selective spectrin deficiency (32). These data support the conclusion (32) that the rate of band 3 lateral diffusion is controlled primarily by the RBC membrane spectrin/band 3 ratio.

The laterally mobile fraction of HS^{ank} band 3 showed no significant correlation ($R^2 = 0.07$) with RBC spectrin/band 3 ratio (Figure 1B). Band 3 fractional mobility was $47 \pm 4\%$ (mean \pm SD, $n = 4$) in normal RBCs, similar to previously reported values (29, 31, 32, 43, 54–56), and $49 \pm 4\%$ ($n = 6$) in HS^{ank} RBCs. Of note, HS^{sp} RBCs with selective spectrin deficiency also exhibited no significant correlation between band 3 fractional mobility and spectrin/band 3 ratio (32).

The polarized fluorescence depletion technique was used to measure the rotational mobility of EMA-labeled band 3. Normal RBCs had three rotationally distinct populations of band 3 molecules (upper curve, Figure 2), including $22 \pm 7\%$ rapidly rotating molecules (τ_1 , $83 \pm 37 \mu\text{s}$), $65 \pm 8\%$ slowly rotating molecules (τ_2 , $2.0 \pm 0.9 \text{ ms}$), and $13 \pm 4\%$ rotationally immobile molecules ($n = 4$ individuals), similar to previously reported values (24, 31, 32, 34, 41, 43, 45, 58). Band 3 rotational mobility in HS^{ank} RBCs differed significantly from that in normal cells. Although the decay of fluorescence anisotropy in normal RBCs required two exponential terms for adequate fitting, in HS^{ank} RBCs the anisotropy decay could be adequately fitted by a single exponential, suggesting primarily one rotationally mobile band 3 population (lower curve, Figure 2). Approximately 80% of band 3 molecules were found to rotate with a single rotational relaxation time, while 20% of band 3 molecules were rotationally immobile. The single rotational relaxation time ranged from 263 to 941 μs (Table 2). Importantly, the rotational relaxation time was highly correlated ($R^2 = 0.81$)

Table 2: Band 3 Rotational Mobility in HS^{ank} RBCs^a

sample	rotationally mobile fraction (%)	rotational relaxation time (μs)	rotationally immobile fraction (%)
patient 1	93	263	7
patient 2	95	350	5
patient 3	72	325	28
patient 4	76	487	24
patient 5	68	672	32
patient 6	75	941	25
average of 6 patients	80 ± 12		20 ± 12

^a Band 3 was fluorescently labeled in intact RBCs with the covalent probe eosin maleimide. Rotational mobility was measured by using the polarized fluorescence depletion technique. HS^{ank} RBCs manifested a single band 3 rotational relaxation time and a rotationally immobile fraction. In comparison, normal RBCs ($n = 4$) exhibited two rotationally mobile populations and an immobile population of band 3 molecules: $22 \pm 7\%$ of molecules had a rotational relaxation time of $83 \pm 37 \mu\text{s}$, $65 \pm 8\%$ of molecules had a rotational relaxation time of $2.0 \pm 0.9 \text{ ms}$, and $13 \pm 4\%$ of molecules were rotationally immobile. When the band 3 rotational mobility of normal RBCs was fitted using a single-exponential decay, the average rotational relaxation time was $946 \pm 137 \mu\text{s}$, and the average rotationally immobile fraction was $30 \pm 9\%$. The latter results are consistent with previous measurements of band 3 rotational mobility performed by Cherry and colleagues (69–71).

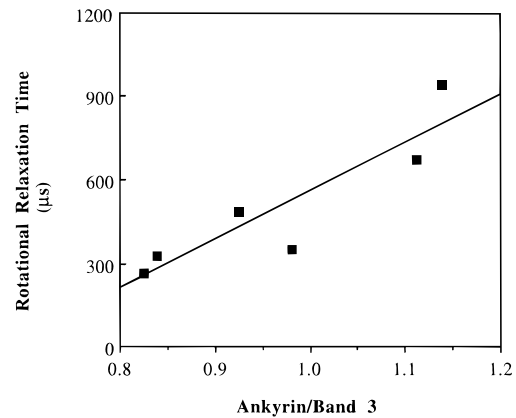


FIGURE 3: Dependence of band 3 rotational relaxation time on normalized ankyrin/band 3 ratio in intact RBCs from HS^{ank} patients. Anisotropy decay curves for the six HS^{ank} RBC samples were analyzed by fitting each curve to a single exponential. Chi-square values ranged from 0.55 to 1.19 for the equations corresponding to the best fit anisotropy decay curves. Equation of best fit was: rotational relaxation time (μs) = $-1179 + 1737$ (ankylin/band 3); $R^2 = 0.81$.

with the ankyrin/band 3 ratio (Figure 3). From the slope of the linear regression line, it was calculated that, on average, a 16% decrease in the ankyrin/band 3 ratio resulted in a 2-fold decrease in τ . Because the predicted value of τ approached 0 for ankyrin/band 3 ratios less than 0.68, it should be noted that the relationship described in Figure 3 could not be extrapolated to ankyrin/band 3 ratios less than 0.8. Compared to band 3 rotational mobility in normal RBCs, the mobility in HS^{ank} RBCs was notable for the disappearance of the slowly rotating band 3 population ($\tau \sim 1\text{--}3 \text{ ms}$). These data suggested that, although a rotationally immobile band 3 population remained in HS^{ank} RBCs, the rotational relaxation time of the slowly rotating band 3 population became comparable to that of the rapidly rotating band 3 population. This effect on band 3 rotational mobility was apparently induced by the ankyrin defect in HS^{ank} RBCs, because the rotational mobility of band 3 in HS^{sp} cells with selective spectrin deficiency was similar to that in normal RBCs (32).

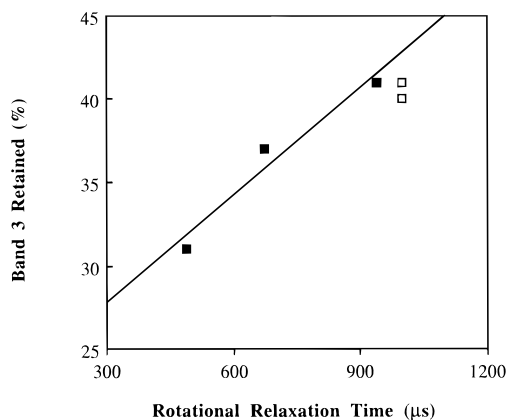


FIGURE 4: Correlation between band 3 rotational relaxation time and band 3 retention in membrane skeletons from HS^{ank} RBCs following extraction by the nonionic detergent C₁₂E₈. Anisotropy decay curves for the three HS^{ank} (filled squares) and two normal (open squares) RBC samples were analyzed by fitting each curve to a single exponential. Band 3 retention in the membrane skeleton was determined as described under Materials and Methods, and expressed as the percent of total band 3 retained in C₁₂E₈-extracted isotonic skeletal shells. The band 3 rotational relaxation time varied directly with the degree to which band 3 was retained in HS^{ank} membrane skeletons following nonionic detergent extraction.

The increased rotational mobility of band 3 in ankyrin-deficient HS^{ank} RBCs suggested that binding interactions between band 3 and ankyrin could represent an important constraint on band 3 rotation. To investigate more directly the degree of association between band 3 and the HS^{ank} membrane skeleton, ghosts prepared from HS^{ank} RBCs were extracted with the nonionic detergent C₁₂E₈. Among the three HS^{ank} and two normal RBC samples examined, there was an inverse correlation between the band 3 rotational relaxation time and the retention of band 3 in the C₁₂E₈-extracted membrane skeleton (Figure 4). This observation provided further support for the hypothesis that binding interactions between band 3 and the membrane skeleton confer significant constraints on band 3 rotational mobility.

DISCUSSION

Band 3 lateral mobility is constrained in normal human RBC membranes by steric hindrance interactions, low-affinity binding interactions, and high-affinity binding interactions (29, 31, 37–40, 45). Steric hindrance interactions between band 3 oligomers and the spectrin-based membrane skeleton provide the major constraint on the laterally mobile band 3 fraction, slowing the rate of band 3 lateral diffusion by approximately 50-fold compared to the predicted diffusion rate of “free” band 3 in membranes devoid of a functional membrane skeleton (29, 30, 32, 37). Our finding that the lateral diffusion coefficient of band 3 is inversely related to the spectrin/band 3 ratio in HS^{ank} RBCs is consistent with the steric hindrance model of lateral mobility regulation. We observe that both the extrapolated intercept (i.e., the diffusion coefficient at a spectrin/band 3 ratio of 0) and the slope of the line relating the logarithm of the band 3 lateral diffusion coefficient to the spectrin/band 3 ratio in HS^{ank} RBCs are similar to those seen in HS^{sp} RBCs (32). Because the intercept represents the predicted diffusion rate of “free” band 3 in the absence of a spectrin-based membrane skeleton, our data are consistent with estimates of the band 3 “rapid diffusion limit” based on studies of biochemically perturbed

normal RBC ghost membranes (29, 30). The present results also extend the range of spectrin/band 3 ratios over which the inverse relationship between band 3 lateral diffusion coefficient and spectrin/band 3 ratio is valid, because the spectrin/band 3 ratios in HS^{sp} RBCs range from 0.43 to 0.74 (32) while those in HS^{ank} RBCs range from 0.73 to 1.18 (the present study). Taken together, then, studies on the lateral mobility of band 3 in biochemically perturbed normal RBCs, HS^{sp} RBCs, and HS^{ank} RBCs suggest that the spectrin/band 3 ratio is the major determinant of the lateral diffusion rate of band 3 over the entire range of ratios from 0 (i.e., in the absence of spectrin) to 1 (i.e., in the normal RBC membrane).

Band 3 rotational mobility is constrained in normal RBC membranes by low-affinity and high-affinity binding interactions (24, 31, 33, 34, 41–45, 58–60). The rotationally immobile band 3 fraction apparently represents individual band 3 molecules bound with high affinity to ankyrin. The rapidly rotating band 3 fraction consists of band 3 species (dimers and possibly tetramers) that are free from rotational constraints other than the viscosity of the lipid bilayer (34, 36). The slowly rotating band 3 fraction is less well-defined. Rotational constraints applied by low-affinity binding interactions between ankyrin-linked band 3 and other band 3 molecules, and between the cytoplasmic domain of band 3 and membrane skeletal proteins such as ankyrin (44, 45), protein 4.1 (15), and protein 4.2 (18, 19, 24), have been invoked. Steric hindrance interactions are not important in constraining band 3 rotational mobility (32). Here we find that relatively modest changes in the RBC ankyrin/band 3 ratio are associated with striking alterations in band 3 rotational mobility, and that the rotational relaxation time obtained using single exponential analysis correlates linearly with the ankyrin/band 3 ratio in HS^{ank} RBCs. We conclude from these data that ankyrin plays a major role in regulating the rotational diffusion of the rotationally mobile band 3 population.

Rotational mobility data can be fitted using two or more exponentials when the rotational relaxation times of the two or more populations of molecules differ substantially. For example, in normal RBC membranes, band 3 rotational relaxation times of <250 μs and 1–3 ms can be discriminated. In RBC ghost membranes, a very short relaxation time of $\sim 25 \mu\text{s}$ can also be observed (34, 61). Thus, an order of magnitude difference in rotational relaxation times allows two or more populations of band 3 molecules to be discriminated. In HS^{ank} RBCs, the band 3 anisotropy decay curves are adequately fitted using a single exponential. This is possible only if all rotationally mobile molecules have relaxation times that are within an order of magnitude of one another. Here we find that the shortest HS^{ank} band 3 rotational relaxation times are closer to the relaxation times of the rapidly rotating band 3 fraction than to those of the slowly rotating band 3 fraction in normal RBCs. It therefore appears that the major consequence of ankyrin deficiency is to increase the speed of rotation of the slowly rotating population of band 3 molecules. The simplest physical interpretation of these data is that low-affinity binding interactions between ankyrin and the cytoplasmic domain of band 3 provide the major constraint on the rotationally mobile population of band 3 molecules.

Although ours are the first measurements of band 3 rotational mobility in ankyrin-deficient intact human RBCs,

the notion that interactions between band 3 and ankyrin are responsible for slowing band 3 rotational diffusion is supported by previous biophysical and biochemical studies. Several investigators have found that proteolytic cleavage of the cytoplasmic domain of band 3 allows increased rotational freedom of band 3 in RBC ghost membranes (33, 34, 62), as does treatment of RBC ghost membranes under pH or ionic strength conditions expected to weaken binding interactions between band 3 and ankyrin (33, 62, 63). Che et al. (63) have shown that binding of ankyrin to band 3 reconstituted into artificial lipid vesicles promotes association of the band 3 into slowly rotating complexes. Thevenin and Low (64) have reported both high-affinity ($K_d \sim 13$ nM) and low-affinity ($K_d \sim 130$ nM) binding interactions between ankyrin and band 3, and Michaely and Bennett (65) have characterized on ankyrin two distinct band 3 binding sites of different affinity (K_d 's ~ 10 and 40 nM, respectively). These data support the interpretation that ankyrin interacts with band 3 in both a high-affinity and a low-affinity interaction.

The most unexpected finding in the present study is the observation that a relatively modest change in ankyrin/band 3 ratio alters the rotational diffusion of the major fraction of band 3 molecules. We offer two hypotheses as possible explanations for this result. First, the state of oligomerization of ankyrin-linked band 3 could be altered in HS^{ank} RBCs. The biosynthetic rate of ankyrin is greater than that of band 3 in the early erythroblast stage of normal erythropoiesis, such that stable molecular complexes between ankyrin monomers and band 3 tetramers form in the endoplasmic reticulum and are inserted as a "cassette" into the plasma membrane. Later in normal erythropoiesis ankyrin biosynthesis ceases but band 3 biosynthesis continues, so that "free" band 3 dimers are inserted into the membrane. Importantly, these ankyrin-linked and "free" populations of band 3 oligomers do not interconvert once they are localized in the plasma membrane (66–68). The rate of ankyrin biosynthesis in HS^{ank} RBCs (excluding patient 6; see refs 46, 48) is likely to be about 50% of that in normal RBCs, because these HS^{ank} RBCs have only one functional ankyrin allele. In early HS^{ank} erythropoiesis, then, about half of the normal complement of ankyrin-linked band 3 tetramers is predicted to reach the plasma membrane. In late HS^{ank} erythropoiesis, although ankyrin biosynthesis is apparently not completely shut off (cf., the ankyrin content of HS^{ank} RBCs is about 80% rather than 50% of that of normal RBCs), the rate of band 3 synthesis is likely to have increased to the point that many "free" band 3 dimers are inserted into the membrane. We postulate, then, that ankyrin synthesized late in erythropoiesis in HS^{ank} RBCs becomes preferentially complexed at the plasma membrane with band 3 dimers rather than band 3 tetramers. There is ample precedent in the literature for the ability of band 3 dimers as well as tetramers to interact with ankyrin [see discussion in Thevenin and Low (64)]. This hypothesized alteration in the stoichiometry of ankyrin/band 3 complexes is supported by the observations that RBCs from patients 4 and 5 exhibit ankyrin/band 3 ratios of 0.93 and 1.11, respectively, but only 76% and 90%, respectively, of the normal amount of band 3 is retained in the C₁₂E₈-extracted membrane skeletons. The predicted effect of this alteration in the state of oligomerization of ankyrin-linked band 3 on measured band 3

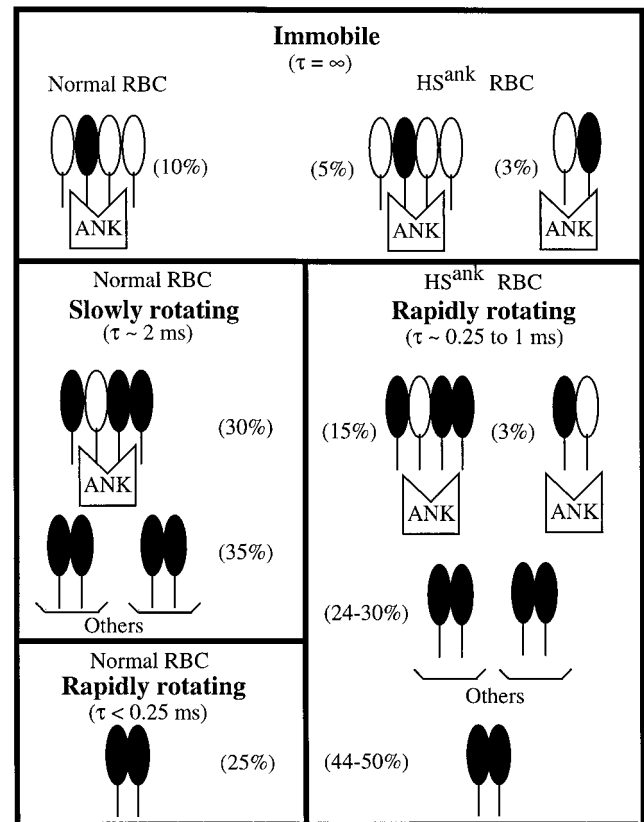


FIGURE 5: Schematic illustration of band 3 populations in normal and HS^{ank} RBCs, assuming that the state of oligomerization of ankyrin-linked band 3 and the association rate for binding between band 3 and membrane skeletal components are both decreased in HS^{ank} compared to normal RBCs (see Discussion). In each panel, the band 3 molecules affected by the designated molecular interaction are shaded. The model assumes that, in a normal RBC, all 100 000 ankyrin molecules are complexed with band 3 tetramers, 25% of band 3 molecules are present as freely rotating dimers, and the remaining band 3 molecules are rotationally slowed by low-affinity binding interactions with ankyrin (30%) and other membrane skeletal components such as protein 4.1 and protein 4.2 (35%). The model also assumes that, in an HS^{ank} RBC, 50 000 ankyrin molecules are complexed with band 3 tetramers and 35 000 ankyrin molecules are complexed with band 3 dimers; and the remaining band 3 molecules are subjected to the same rotational constraints as those in normal RBCs, with the notable exceptions that HS^{ank} RBCs are deficient in other membrane skeletal components as well as ankyrin, and that the low-affinity binding interactions between band 3 and membrane skeletal components are 10-fold weaker in HS^{ank} RBCs. In normal RBCs, then, 10% of band 3 molecules are predicted to be rotationally immobilized by binding with high affinity to ankyrin; 25% are expected to rotate rapidly as "free" dimers; and the remaining 65% are predicted to rotate slowly. In HS^{ank} RBCs, 8% of band 3 molecules are predicted to be rotationally immobilized by binding with high affinity to ankyrin (comprising 5% of molecules present in tetramer and 3% in dimer form); and the remaining 92% of molecules are expected to rotate rapidly as molecular species that are affected by weak low-affinity binding interactions with ankyrin (18%), affected by weak low-affinity binding interactions with other membrane skeletal components (24–30%), or rotating freely as band 3 dimers (44–50%). These shifts in the proportions of band 3 molecules in the rapidly and slowly rotating populations, and in the rotational relaxation time of the slowly rotating band 3 population, result in a marked increase in the average rotational diffusion rate in HS^{ank} compared to normal RBCs.

rotational diffusion rates is illustrated schematically in Figure 5.

A decrease in the average state of oligomerization of ankyrin-linked band 3 could account for a shift in HS^{ank} RBCs from the slowly rotating to the rapidly rotating population of band 3 molecules, but this effect would not explain the observed increase in the speed of rotation of the slowly rotating population. To address this issue, our second hypothesis is that the decreased number of contacts between the membrane skeleton and the overlying lipid bilayer in ankyrin-deficient HS^{ank} RBCs results in a decreased efficiency of physical coupling between the skeleton and the overlying bilayer (see ref 67). Weakening of this coupling could decrease the effective concentrations of ankyrin and band 3 in the three-dimensional space between the plane of the membrane skeleton and the inner leaflet of the membrane bilayer, and thereby decrease the association rate for the ankyrin–band 3 binding interaction. For example, a 10-fold decrease in the association rate could cause a 10-fold increase in the speed of rotation of the slowly rotating band 3 population, so that this population would become indistinguishable from the rapidly rotating population. Similar considerations would be expected to decrease the association rate for the binding interactions between band 3 and other membrane skeletal components such as protein 4.1 and protein 4.2 (see Figure 5).

In the present study, there was no significant correlation between either the laterally or the rotationally immobile fraction of band 3 and the RBC spectrin/band 3 ratio or the ankyrin/band 3 ratio. At first glance this lack of correlation is surprising, because high-affinity binding interactions between ankyrin and band 3 tetramers [or “pseudotetramers” (65)] are thought to be the major molecular mechanism responsible for immobilization of band 3. One resolution to this apparent paradox could be that HS^{ank} RBCs are not only ankyrin deficient but also band 3 deficient. Alternatively, membranes of HS^{ank} RBCs could contain band 3 with different patterns of oligomerization states (i.e., dimers, tetramers, and higher order oligomers) than those in normal RBCs (see above). Finally, it could be the case that the experimentally measured laterally and rotationally immobile fractions are not determined with sufficient precision to allow discrimination of a small but significant difference between band 3 immobile fractions in normal and HS^{ank} RBCs.

In conclusion, studies on intact ankyrin-deficient human RBCs suggest that low-affinity binding interactions between band 3 and ankyrin provide the chief constraint to the rotational mobility of band 3 in its native membrane environment. This conclusion complements earlier work showing that steric hindrance interactions between band 3 and spectrin represent the primary constraint to band 3 lateral mobility. Band 3 is therefore the first integral membrane protein for which the major forces constraining lateral and rotational mobility have been determined at the molecular level.

ACKNOWLEDGMENT

We are grateful to the patients and controls for donating blood samples. We thank Carrie Armsby for careful handling of blood samples and Patrick Yacono for excellent technical assistance.

REFERENCES

- Steck, T. L. (1974) *J. Cell Biol.* 62, 1–19.
- Gardner, K., and Bennett, G. V. (1989) in *Red Blood Cell Membranes: Structure, Function and Clinical Implications* (Agre, P., and Parker, J. C., Eds.) pp 1–29, Marcel Dekker, New York.
- Lux, S. E., and Palek, J. (1995) in *Blood: Principles and Practice of Hematology* (Handin, R. L., Lux, S. E., and Stossel, T. P., Eds.) pp 1701–1818, J. B. Lippincott, Philadelphia, PA.
- Low, P. S. (1986) *Biochim. Biophys. Acta* 864, 145–167.
- Low, P. S., Willardson, B. M., Mohandas, N., Rossi, M., and Shohet, S. (1991) *Blood* 77, 1581–1586.
- Anstee, D. J., Hemming, N. J., and Tanner, M. J. (1995) *Immunol. Invest.* 24, 187–198.
- Discher, D. E., Winardi, R., Schischmanoff, P. O., Parra, M., Conboy, J. G., and Mohandas, N. (1995) *J. Cell Biol.* 130, 897–907.
- Mohandas, N., and Evans, E. (1994) *Annu. Rev. Biophys. Biomol. Struct.* 23, 787–818.
- Cabantchik, Z. I., and Rothstein, A. (1974) *J. Membr. Biol.* 15, 207–226.
- Ho, M. K., and Guidotti, G. (1975) *J. Biol. Chem.* 250, 675–683.
- Tanner, M. J. (1993) *Bailliere's Clin. Haematol.* 6, 333–356.
- Bennett, V., and Stenbuck, P. J. (1980) *J. Biol. Chem.* 255, 6424–6432.
- Hargreaves, W. R., Giedd, K. N., Verkleij, A. V., and Branton, D. (1980) *J. Biol. Chem.* 255, 11965–11972.
- Reithmeier, R. A. F. (1993) *Curr. Opin. Struct. Biol.* 3, 515–523.
- Pasternack, G. R., Anderson, R. A., Leto, T. L., and Marchesi, V. T. (1985) *J. Biol. Chem.* 260, 3676–3683.
- Lombardo, C. R., Willardson, B. M., and Low, P. S. (1992) *J. Biol. Chem.* 267, 9540–9546.
- Yu, J., and Steck, T. L. (1975) *J. Biol. Chem.* 250, 9176–9184.
- Korsgren, C., and Cohen, C. M. (1986) *J. Biol. Chem.* 261, 5536–5543.
- Korsgren, C., and Cohen, C. M. (1988) *J. Biol. Chem.* 263, 10212–10218.
- Tyler, J. M., Reinhardt, B. N., and Branton, D. (1980) *J. Biol. Chem.* 255, 7034–7039.
- Kennedy, S. P., Warren, S. L., Forget, B. G., and Morrow, J. S. (1991) *J. Cell Biol.* 115, 267–277.
- Platt, O. S., Lux, S. E., and Falcone, J. F. (1993) *J. Biol. Chem.* 268, 24421–24426.
- Schischmanoff, P. O., Winardi, R., Discher, D. E., Parra, M. K., Bicknese, S. E., Witkowska, H. E., Conboy, J. G., and Mohandas, N. (1995) *J. Biol. Chem.* 270, 21243–21250.
- Golan, D. E., Corbett, J. D., Korsgren, C., Thatte, H. S., Yawata, Y., and Cohen, C. M. (1996) *Biophys. J.* 70, 1534–1542.
- Singer, S. J., and Nicholson, G. L. (1972) *Science* 175, 720–731.
- Nicholson, G. L. (1976) *Biochim. Biophys. Acta* 457, 57–108.
- Jacobson, K., Ishihara, A., and Inman, R. (1987) *Annu. Rev. Physiol.* 49, 163–175.
- Jacobson, K., Sheetz, E. D., and Simson, R. (1995) *Science* 268, 1441–1442.
- Golan, D. E., and Veatch, W. (1980) *Proc. Natl. Acad. Sci. U.S.A.* 77, 2537–2541.
- Golan, D. E. (1989) in *Red Blood Cell Membranes: Structure, Function and Clinical Implications* (Agre, P., and Parker, J. C., Eds.) pp 367–400, Marcel Dekker, New York.
- Corbett, J. D., and Golan, D. E. (1993) *J. Clin. Invest.* 91, 208–217.
- Corbett, J. D., Agre, P., Palek, J., and Golan, D. E. (1994) *J. Clin. Invest.* 94, 683–688.
- Nigg, E. A., and Cherry, R. J. (1980) *Proc. Natl. Acad. Sci. U.S.A.* 77, 4702–4706.
- Matayoshi, E. D., and Jovin, T. M. (1991) *Biochemistry* 30, 3527–3538.
- Cherry, R. J. (1992) in *Structural and Dynamic Properties of Lipids and Proteins* (Quinn, P. J., and Cherry, R. J., Eds.) pp 137–152, Portland Press, London.

36. Mühlebach, T., and Cherry, R. J. (1985) *Biochemistry* 24, 975–983.
37. Sheetz, M. P., Schindler, M., and Koppel, D. E. (1980) *Nature* 285, 510–512.
38. Fowler, V., and Bennett, V. (1978) *J. Supramol. Struct.* 8, 215–221.
39. Koppel, D. E., Sheetz, M. P., and Schindler, M. (1981) *Proc. Natl. Acad. Sci. U.S.A.* 78, 3576–3580.
40. Tsuji, A., and Ohnishi, S. (1986) *Biochemistry* 25, 6133–6139.
41. Tilley, L., Nash, G. B., Jones, G. L., and Sawyer, W. H. (1991) *J. Membr. Biol.* 121, 59–66.
42. Che, A., Cherry, R. J., Bannister, L. H., and Dluzewski, A. R. (1993) *J. Cell Sci.* 105, 655–660.
43. Liu, S.-C., Palek, J., Yi, S. J., Nichols, P. E., Derick, L. H., Chiou, S. S., Amato, D., Corbett, J. D., Cho, M. R., and Golan, D. E. (1995) *Blood* 86, 349–358.
44. Wyatt, K., and Cherry, R. (1992) *Biochim. Biophys. Acta* 1103, 327–330.
45. Tsuji, A., Kawasaki, K., Ohnishi, S., Merkle, H., and Kusumi, A. (1988) *Biochemistry* 27, 7447–7452.
46. Eber, S. W., Gonzalez, J. M., Lux, M. L., Scarpa, A. L., Tse, W. T., Dornwell, M., Herbers, J., Kugler, W., Özcan, R., Pekrun, A., Gallagher, P. G., Schröter, W., Forget, B. G., and Lux, S. E. (1996) *Nat. Genet.* 13, 214–218.
47. Lux, S. E., Tse, W. T., Menninger, J. C., John, K. M., Harris, P., Shalev, O., Chilcote, R. R., Marchesi, S. L., Watkins, P. C., Bennett, V., McIntosh, S., Collins, F. S., Francke, U., Ward, D. C., and Forget, B. G. (1990) *Nature* 345, 736–739.
48. Pekrun, A., Eber, S. W., Kuhlmeier, A., and Schröter, W. (1993) *Ann. Hematol.* 67, 89–93.
49. Axelrod, D., Koppel, D. E., Schlessinger, J., Elson, E., and Webb, W. W. (1976) *Biophys. J.* 16, 1055–1069.
50. Bevington, P. R. (1969) *Data reduction and error analysis for the physical sciences*, McGraw-Hill Inc., New York.
51. Yoshida, T. M., and Barisas, B. G. (1986) *Biophys. J.* 50, 41–53.
52. Johnson, P., and Garland, P. B. (1981) *FEBS Lett.* 132, 252–256.
53. Agre, P., Casella, J. F., Zinkham, W. H., McMillan, C., and Bennett, V. (1985) *Nature* 314, 380–383.
54. Jarolim, P., Rubin, H. L., Liu, S.-C., Cho, M. R., Brabec, V., Derick, L. H., Yi, S., Saad, S. T. O., Alper, S., Brugnara, C., Golan, D. E., and Palek, J. (1994) *J. Clin. Invest.* 93, 121–130.
55. Liu, S.-C., Zhai, S., Palek, J., Golan, D. E., Amato, K., Hassan, G., Nurse, T., Babona, D., Coetzer, T., Jarolim, P., Zaik, M., and Borwein, S. (1990) *N. Engl. J. Med.* 323, 1530–1538.
56. Mohandas, N., Winardi, R., Knowles, D., Leung, A., Parra, M., George, E., Conboy, J., and Chasis, J. (1992) *J. Clin. Invest.* 89, 686–692.
57. Schindler, M., Koppel, D. E., and Sheetz, M. P. (1980) *Proc. Natl. Acad. Sci. U.S.A.* 77, 1457–1461.
58. Clague, M. J., Harrison, J. P., and Cherry, R. J. (1989) *Biochim. Biophys. Acta* 981, 43–50.
59. Nigg, E. A., and Cherry, R. J. (1979) *Nature* 277, 493–494.
60. Sakaki, T., Tsuji, A., Chang, C. H., and Ohnishi, S. (1982) *Biochemistry* 21, 2366–2372.
61. McPherson, R. A., Sawyer, W. H., and Tilley, L. (1992) *Biochemistry* 31, 512–518.
62. McPherson, R. A., Sawyer, W. H., and Tilley, L. (1993) *Biochemistry* 32, 6696–6702.
63. Che, A., Morrison, I. E. G., Pan, R., and Cherry, R. J. (1997) *Biochemistry* 36, 9588–9595.
64. Thevenin, B. J., and Low, P. S. (1990) *J. Biol. Chem.* 265, 16166–16172.
65. Michaely, P., and Bennett, V. (1995) *J. Biol. Chem.* 270, 22050–22057.
66. Gomez, S., and Morgans, C. (1993) *J. Biol. Chem.* 268, 19593–19597.
67. Yi, S. J., Liu, S.-C., Derick, L. H., Murray, J., Barker, J. E., Cho, M. R., Palek, J., and Golan, D. E. (1997) *Biochemistry* 36, 9596–9604.
68. Hanspal, M., Golan, D. E., Smockova, Y., Yi, S. J., Cho, M. R., Liu, S.-C., and Palek, J. (1998) *Blood* 92, 329–338.
69. Cherry, R. J., Bürkli, A., Busslinger, M., Schneider, G., and Parish, G. R. (1976) *Nature* 263, 389–393.
70. Cherry, R. J. (1979) *Biochim. Biophys. Acta* 559, 289–327.
71. Cherry, R. J., and Nigg, E. (1979) *Prog. Clin. Biol. Res.* 30, 475–481.

BI981825C